

# Effect of Interface Modification on the Mechanical Behavior of Carbon Nanotube Reinforced Composites Using Parallel Molecular Dynamics Simulations

S. Namilae<sup>1</sup>, U. Chandra<sup>2</sup>, A. Srinivasan<sup>3</sup> and N. Chandra<sup>4</sup>

**Abstract:** Molecular dynamics (MD) simulations play an important predictive role in understanding the behavior of nanoscale systems. In this paper, parallel MD simulations are used to understand the mechanical behavior of interfaces in CNT based composites. We present an algorithm for parallel implementation of MD simulations of carbon nanotube (CNT) based systems using reactive bond order potentials. We then use that algorithm to model the CNT-polymer interfaces with various levels of interaction as (a) described only by long range Van Der Waals interactions (b) chemically bonded with fixed matrix and (c) chemically bonded with matrix explicitly modeled. It is shown that interface strength based on non bonded interactions is very low (of the order of few MPa) and it can be significantly improved through surface chemical modification of CNTs (to an order of a few GPa). It is further noted that chemical bonding between functionalized nanotube and matrix during processing is essential to obtain good interface strength and hence a better composite.

**Keyword:** Carbon nanotube composites, interfaces, parallel molecular dynamics.

## 1 Introduction

Computational simulations play an important predictive role in the study of nanoscale systems, especially because of the difficulties associated with

controlled experimentation at nano-scale. For example, consider the interfacial load transfer behavior in CNT based composites. Both experimental and computational studies have clearly established that fiber-matrix interfaces play a key role in determining the strength, stiffness and fracture resistance of composites. The role of interfaces in nanocomposites is quite substantial since in this case the interface/volume ratio is significantly higher. Difficulties with controlled experimentation (both specimen preparation and property measurement) at nanometer scale have often resulted in contradicting observations and conclusions regarding interface strength. Computational simulation based on MD is an ideal technique to understand such problems related to mechanical behavior at atomic scales.

Carbon nanotubes are known to possess better mechanical properties such as strength of about 150 GPa (Demczyk 2003), stiffness of 1 TPa (Treacy 1996, Chandra 2004 and references therein) than any other fiber or reinforcement known to mankind. They are known to be extremely resilient under elastic deformation and have the ability to absorb large amounts of strain energy (Yakobson 1996, Namilae 2006). In addition, they possess excellent thermal conductivity (6000W/m/K) (Ling 2006) and unique electrical properties (Saito 2001). These combinations of mechanical and physical properties make them ideal reinforcements for both structural and multifunctional applications. In order to achieve desired mechanical properties in composites, it is not only necessary that the constituent phases (fiber and matrix) have good mechanical properties but also essential that fibers be properly aligned, uniformly distributed and more importantly have good interfacial load transfer proper-

<sup>1</sup> Oak Ridge National Laboratory, Oak Ridge, TN 37831

<sup>2</sup> Department of Computer and Information Sciences, Florida A&M University, Tallahassee, FL, 32307

<sup>3</sup> Department of Computer Science, Florida State University, Tallahassee, FL, 32306

<sup>4</sup> Department of Engineering Mechanics, University of Nebraska-Lincoln, Lincoln, NE 68588

Table 1: Experimentally reported elastic moduli of nanotube composites compared with simplistic maxima and minima based on series and parallel models. Commercial values of density are used in calculations if not provided in the references.

Researcher	Matrix	Vol or Wt% CNT	Exptl $E_C/E_M$	Calculation $E_C/E_M$	
				Parallel	Series
Schaddler '98 [11]	Epoxy	5 Wt%(tension)	1.13	9.60	1.03
	Epoxy	5 Wt% (comp)	1.4	9.60	1.03
Andrews '99 [13]	Petroleum pitch	1 Wt%	1.20	9.09	1.003
		5 Wt%	2.29	12.46	1.016
Gong '00 [14]	Epoxy	1 Wt%	1.12	4.98	1.0057
		1Wt%	1.25	4.98	1.0057
		(With surfactant)			
Qian '00 [7]	Polystyrene	1 Wt%	1.24	4.9151	1.0049
Andrews'02 [15]	Polystyrene	2.5 (vol%)	1.22	14.86	1.03
		5.0	1.28	28.73	1.05
		10.0	1.67	56.46	1.11
		15.0	2.06	84.18	1.18
		25.0	2.50	139.64	1.33
	PPA	0.50(vol%)	1.17	5.16	1.01
		1.50	1.33	13.49	1.02
		2.50	1.50	21.81	1.03
		5.00	2.50	42.62	1.05
Allaoui'02 [16]	Rubber- Epoxy resin	1 Wt%	2.0	49.299	1.006
		2 Wt%	3.9	194.198	1.023
Tang '03 [17]	High density Polyethene	1 Wt%	1.034	8.503	1.005
		3 Wt%	1.054	25.309	1.015
		5 Wt%	1.075	42.114	1.026
Bin '03 [18]	Ultra high Molecular wt Polyethene	10 Wt%	1.71	2.379	1.051
		15 Wt%	3.42	4.068	1.078
Gonjy '04 [19]	Epoxy	0.1 Wt%	1.018	1.173	1.001
		0.1 Wt%	1.066 <sup>With</sup>	1.173	1.001
		1 Wt%	1.079 <sup>NH<sub>2</sub></sup>	2.727	1.006

ties. In the case of nanotube reinforcements, there are significant problems related to dispersion and interface load-transfer which have to be overcome before the potential of CNT fibers can be realized to the full extent. We address the issue of interface behavior in this paper. There are conflicting reports regarding the strength of interfaces; several researchers report evidence for load transfer based on microstructural and spectroscopic observations (Qian 2000, Jia 1999, Cooper 2001, 2002); on the contrary some investigators report low interfacial load transfer (Schadler 1998, Ajayan 2000, Andrews 1999). Table 1 compares the experimental values of stiffness measured in some nanotube reinforced composites with theoretical maxima and minima based on parallel (iso-strain) and series (iso-stress) models. The table reveals that the experimental values are much closer to the lower bound (series model) and much less than theoretically possible upper bound (parallel model). While this may be due to lack of alignment, lack of interfacial load transfer could be an important factor and has to be clearly understood. One of the suggested means to improve the mechanical properties of CNT-matrix interfaces is by functionalization of nanotubes.

Functionalization or surface chemical modification of CNTs with various chemical groups such as hydrocarbons, esters, amides, carbonyl groups etc (Gonjy 2004, Michelson 1996, Pekker 2001, Khare 2002, Chen 1998) is expected to improve the mechanical properties of nanotubes by increasing the bond strength between nanotubes and matrix (Namilaee 2004, 2005, Park 2006). In order to improve the composite properties the modified surface of CNT should also effectively bond with the matrix in the composite. These issues regarding the atomic scale interface behavior can be understood using MD simulations.

While MD simulations can clearly provide a wealth of information on the interface behavior, they consider all the atomic degrees of freedom and operate with a time step of less than a femto second. Sequential computing naturally consumes significant effort even for limited system sizes and meaningful time periods of simulation. For example, to understand a system

behavior for even a  $100 \text{ nm}^3$  of material for one nanosecond, it requires five million iterations (time step 0.2 femto seconds) for about a million atoms. The computational effort is further increased when chemical interactions are required to be modeled accurately using complex multi-body potentials such as Tersoff Brenner bond order potential (Brenner 1991, 2002) used in this work. For example, a problem involving the pull-out of a CNT with 3000 atoms for 800,000 time steps takes about two days of computational time on a 2GHz single processor PC running Linux. It is therefore untenable to perform these simulations without the use of effective parallelization.

Spatial parallelization of MD with reactive bond order type potentials presents unique difficulties. For studying mechanical behavior at nanoscale by modeling problems like fiber pullout, MD simulations often involve lower number of atoms (e.g. 3000-10000) and long simulation times (millions of time steps). In such cases, conventional spatial decomposition techniques often lead to fine granularity (less number of atoms per processor) resulting in high communication overhead. Thus more care needs to be taken in the implementation of the parallel code to ensure that communication does not become a bottleneck. In section 2, we present parallelization algorithms to address these issues for large scale CNT-polymer composite simulations.

We then use parallel MD to study the mechanical behavior of interfaces. Section 3 deals with interface behavior of idealized weak and strong interfaces. These interfaces correspond to situations (i) when there are no chemical attachments between matrix and CNT and (ii) when there are chemical bonds between matrix and CNT and the load is entirely transferred to the matrix. In section 4, the effect of processing on the interface chemistry is studied using a functionalized CNT embedded in polymer matrix. Our parallelization algorithm enables to model a complex science problem with ease. The interface strength of these realistic interfaces is then studied followed by summary and conclusions.

## 2 Parallelization of MD Simulations

The sequential algorithm for a typical MD simulation consists of (a) neighbor list evaluation (b) force computation (c) numerical integration and (d) enforcing the boundary conditions including thermostats. Computational effort for the simulation is generally the highest for neighbor list calculations as they require  $O(N^2)$ . For relatively complicated potentials such as Tersoff-Brenner bond order potential (See Equation (1)) used in this work, the computational effort for force calculations is also significant. This potential accounts for two, three and four body interactions through a bond order term  $B_{ij}$  in the equation (1). The attractive and repulsive portions ( $V_R$  and  $V_A$ ) of the potential are based on Morse exponential potential.

$$E_i = \sum_{j(j \neq i)} [V_R(r_{ij}) + B_{ij}V_A(r_{ij})] \quad (1)$$

This potential has the ability to model chemical bonding and bond conjugation which is critical to the present study. Effective parallelization approach should consider these aspects.

There has been considerable effort in parallelizing MD codes for CNT applications (Ma 2006). Srivastava (1997) used a lexical decomposition method to parallelize the computations on a shared memory machine. Here, the atoms are divided equally amongst the processors based on their indices, thus balancing the load. The speedup reached in these computations was around 16 on 32 processors, with over 2500 atoms per processor. Caglar (2000) performed parallelization using a cell-based decomposition. Atoms are placed in cells and blocks containing equal numbers of adjacent cells are then assigned to different processors. Caglar obtained good speedups with granularity of less than 1000 atoms per processor, however, the performance of the baseline sequential code used to measure speedup was quite slow (about thirty times slower than our baseline sequential code).

Both Srivastava (1997) and Caglar (2000) improve the neighbor list calculation by using a cell-based approach. The spatial domain studied is divided into a number of cells, with the length of a

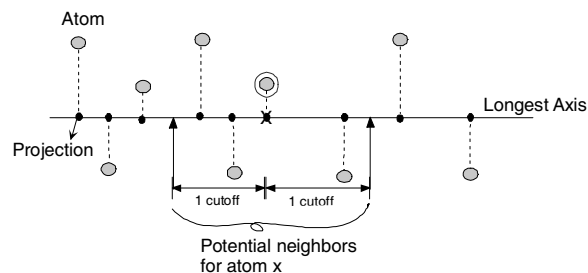


Figure 1: Schematic of the projection-based approach to neighbor list computation.

cell equal to the appropriate cutoff distance. In order to determine the neighbors of an atom, while creating the neighbor list, one needs to search only neighboring cells, as a result the time complexity of computing the neighbor list is  $O(N)$ . The disadvantage of the cell-based algorithm is large memory usage for sparsely populated regions, further; it is less efficient than an array-based representation as it uses indirection, due to access through pointers.

We address these problems by observing that the CNT calculations involve long, thin regions in space. We project the coordinates of the atoms along the axis of longest dimension (z-axis), and then sort the atoms using *insertion sort* based on this projection, as shown in Fig. 1. Neighbors of an atom can be determined by traversing this sorted array on both sides for a length of the cutoff distance. This not only avoids waste of memory, but also facilitates an array representation. While the worst-case time complexity is  $O(N^2)$ , in practice, it only takes  $O(N)$  time since atoms change positions infrequently. We found that the average time for sorting and computing the neighbor list is approximately a half that of the cell-based approach. Sorting also reduces the chances for cache misses.

The parallel algorithm developed in this work is shown in Fig. 2. The design of the parallel code aims to achieve a good speedup with a fine granularity even for a complex geometric domain. We decompose the domain based on the projections along the longest axis, as shown in Fig. 3. The processors can be logically considered as a linear array having two neighbors each (except at the

two ends). The data of the sorted atoms is divided equally into blocks of  $N/P$  atoms, and each block is assigned to a different processor. Though the initial sorting takes significant time, subsequent sorting being local operations, consumes much less time. Each processor also needs the data for the atoms in a buffer region owned by the adjacent processors. The buffer region comprises atoms that are within the three times the cut-off distances (third neighbor) for the border atoms, and every processor exchanges this buffer data with its immediate neighbor (except for the end processors).

A neighbor list computation for the local and buffer atoms is performed on a processor as discussed earlier, but based only on changes in positions of its local atoms. Also, if a neighboring processor performs a neighbor list computation, then the atoms in the buffer regions are sorted, and the neighbor list is recomputed. This is needed to ensure that neighboring processors have a consistent view of atoms they own. When a neighbor list computation is required due to local changes, a processor informs the neighbors of this, along with the message that sends the boundary data, so that the neighbors too can recompute their lists.

```

Initialization
Read input, Sort data for atoms,
Each proc. decides its domain & buffer
Loop over n time steps
- Send and receive buffer data
- Determine neighbor list for
local and buffer atoms (if needed)
  - For each local atom
    Compute two-body forces
    Compute three-body forces
    Compute four-body forces
  Find new positions & velocities
    - Compute potential & kinetic energies
      (Reduction)
  - Apply thermostat: change velocities
  Verify relative motion of atoms;
    if > cut-off then sort data
Endloop

```

Figure 2: Parallel algorithm for MD simulation of CNT Interface.

This scheme assumes that atoms stored in each processor (other than the end processors) span a range of at least three cut-offs, in order to ensure correctness.

We have implemented the parallel code on Dell Xeon 16-node (2 processors per node) and solved the problems related to CNT composites which will be discussed in following sections. Our MD simulations are performed at a constant temperature, which implies that the thermostat needs to be applied at every time step. Maintaining a constant temperature requires computing the global energies, which normally needs a reduction in the parallel code. An *allreduce* operation in a parallel environment combines values from all the processes and distributes the result back to all the processes and hence is expensive in terms of communication cost. Global operations are also required to output certain global values such as total energy. The speedup for the different MD runs for a 7000 atom CNT is shown in Fig. 4 and the computational effort involved in the various segments of the code is shown in Fig. 5.

The speedup curves show that we can get efficient performance on these computations, even with sufficiently fine granularity. The performance of the parallel code can be improved by using local thermostating and by eliminating the *global allreduce* operation. We now use the parallel MD simulations to study the interfacial behavior of CNT based composites.

### 3 Interface Behavior in Idealized Weak and Strong Interfaces

Interface in general can be defined as a region that separates two distinct bodies. Interfaces in composites play a key role in the load distribution between matrix and reinforcement. Interfaces in conventional composites have been modeled using different continuum based methods. For example, they have been modeled as graded continuum (Carman 1993), spring elements (Ananth 1995) and using cohesive zone models (Chandra 2002). However there is a fundamental distinction between interfaces in continuum and atomic scale.

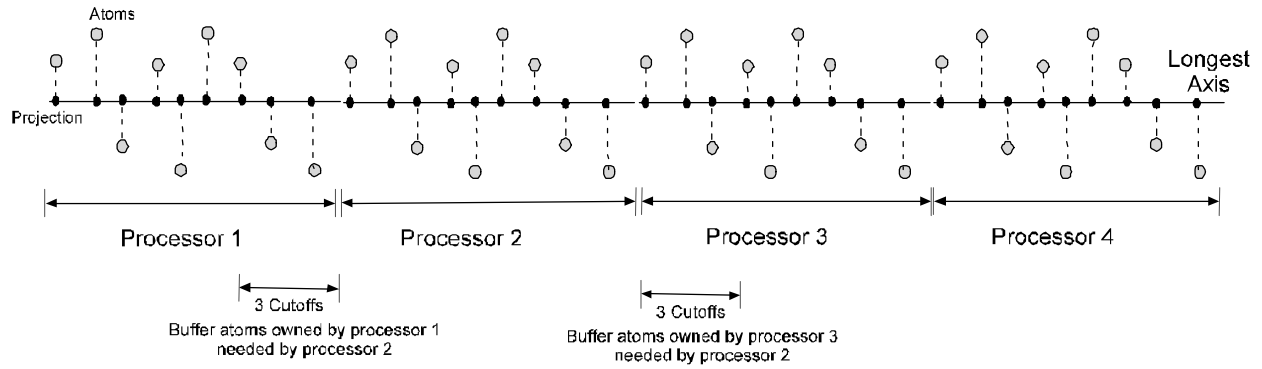


Figure 3: Parallelization using sorted projections.

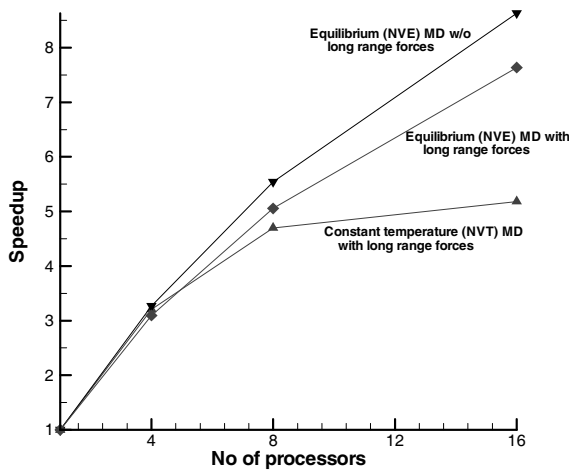


Figure 4: Speedup for various MD Runs.

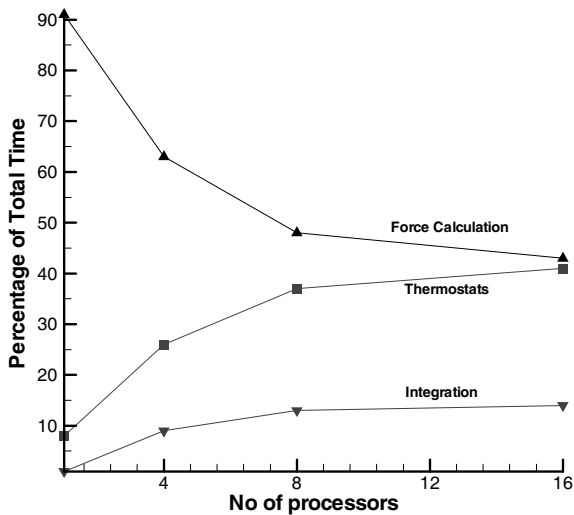


Figure 5: Percent timing in various parts of the parallel code for isothermal run.

Consider two bodies  $\Omega_1$  and  $\Omega_2$  (say fiber and matrix) composed of discrete atoms interacting based on an interatomic potential and separated by an interfacial region  $\gamma$  as shown in Fig. 6. The concept of surface is not clearly defined in a system consisting of discrete particles. Surface here can be considered as an envelope of atoms bounding a predefined region. Based on this idea the interface  $\gamma$  between the two bodies may be considered as region bounded by two surfaces belonging to  $\Omega_1$  and  $\Omega_2$ . This definition of interface as region between two surfaces can be extended to continuum description as well. However, unlike in continuum description the interfacial region in an atomic sense can be composed of a region without any material (or atoms). The interface here would essentially be described by the forces exerted between the two bodies ( $\Omega_1$  and  $\Omega_2$ ) and may or may not consist of any atoms.

In this context, the atomic scale interfaces in nanotube composites can be of two types (i) Interfaces in which the forces are weak Van Der Waals forces only (the interface region here does not contain any atoms) and (ii) Interfaces which are composed of chemical bonds between the matrix and fiber (interface here contains atoms which form the chemical bonds). Van Der Waals forces between any two bodies arise primarily due the attractive forces between the opposite poles of the two bodies, temporarily or permanently created due to electrostatic charge separation (e.g. dipole) in an otherwise neutral atom. This dipole-dipole interaction is typically very weak and temporary and as a result very weak.

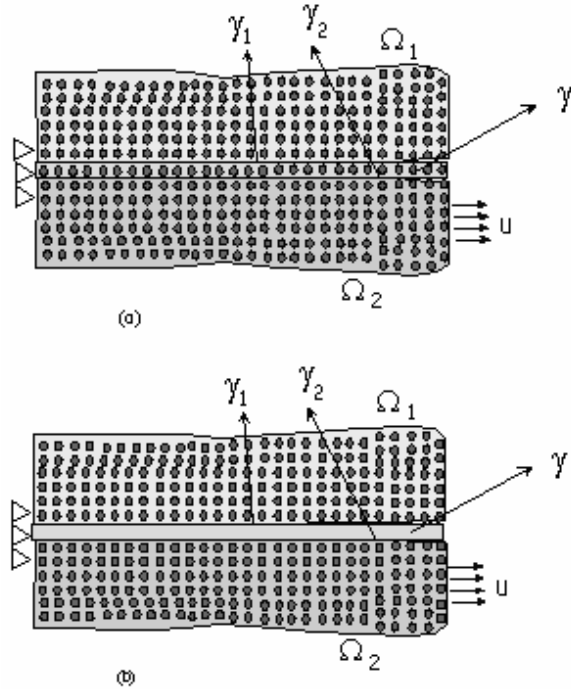


Figure 6: Schematic of atomic scale interfaces.

Contrast this to chemical bonds which are caused by much stronger electron orbital sharing (covalent) or electron transfer (ionic) materials with concomitant release/attraction of energy. The bond strength of covalent chemical bonds is thus very high compared to Van Der Waals interactions. This results in significantly higher interface strength when chemical bonds are involved. In spite of the chemical bonding the interface strength can vary depending upon the fraction of load transmitted to the matrix. We now study the idealized weak interfaces composed of Van Der Waals bonds alone and idealized strong interfaces with chemical bonding and complete load transfer to matrix.

While the C-C and C-H interactions are described by Brenner's potential (1991, 2002), non bonded interactions between carbon atoms are modeled based on Lennard Jones potential given by the equation (2) with  $\varepsilon = 2.86$  meV and  $\sigma = 3.4$  Å (Girifalco 2000).

$$V(r) = 4\varepsilon \left( \left( \frac{\sigma}{r} \right)^{12} - \left( \frac{\sigma}{r} \right)^6 \right) \quad (2)$$

Fiber pullout and push-out tests are typically used

to study the interfacial properties of conventional fiber composites. First, we use molecular statics to study the energetics of nanotube pullout in the three configurations shown in Fig. 7. The configuration of the composite shown in Fig. 7a consists of a (10,10) CNT embedded in a crystalline polymer matrix consisting of 58 polyethene strands. Fig. 7b consists of a bundle of seven (10,10) CNTs and Fig. 7c is (15,15), (10,10) double wall CNT.

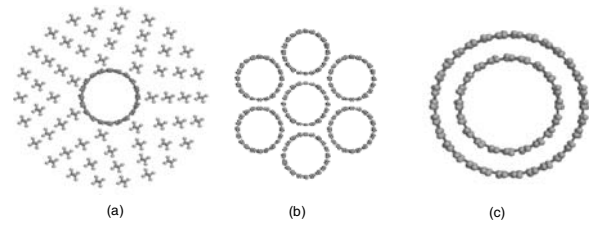


Figure 7: Various configurations for calculation of energy in pullout tests.

Intermediate energetically stable states in pullout test are obtained by sequentially displacing the central nanotube followed by energy minimization. The change in energy vs. displacement plots obtained for the configurations in Fig. 7 are shown in Fig. 8. The energy value reaches a plateau when the nanotube no longer interacts with surroundings and is dependent on the length of the nanotubes. The slope of this Energy-displacement plot is indicative of the interfacial interaction between the nanotubes in bundle. An estimate of interfacial shear strength can be obtained as

$$\sigma_{int} = \frac{1}{A_{CNT}} \left( \frac{\partial(\Delta E)}{\partial r} \right) \quad (3)$$

The interface strength calculated from above equation is 12.5 MPa, 26.6 MPa and 45 MPa for the composite, bundle and multiwall nanotube respectively. This clearly emphasizes that Van Der Waals interactions between nanotube-matrix are extremely low and cannot result in good composites unless the interface strength is improved. In the case of bundles (Fig. 7b) the estimate of the interfacial stress of 26.6 MPa is a very low value

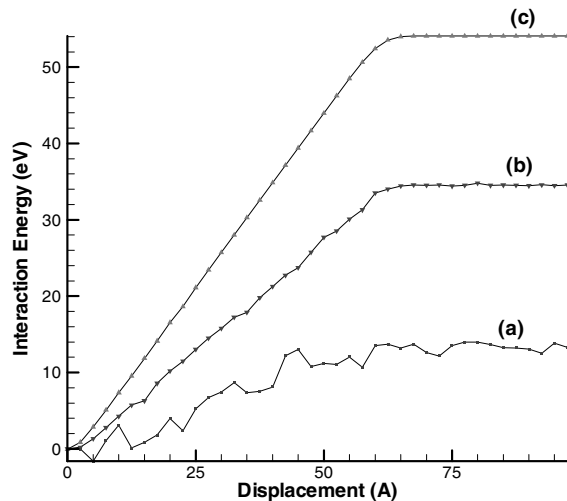


Figure 8: Comparison of interaction energies for bundle of nanotube with multiwall CNT and single wall CNT embedded in polymeric composite.

compared to the reported values of strength (order of a few hundred GPa) of CNTs. This indicates that bundles are much weaker than individual CNTs. The interaction energy and the interface strength (Fig. 8 plot c) are clearly higher for multiwall nanotubes. The sharper oscillations in plot (a) of Fig. 8 are due to sharper changes in configuration due to presence of hydrogen atoms.

It must be mentioned that the interface strength due to Van Der Waals interactions clearly depends on the number of matrix atoms interacting with the embedded CNT. This can be improved by increasing the wrapping of the polymer around CNT. However, the interface strength due to long range interactions will at best be of the order of that in double wall nanotube. These arguments clearly indicate that the only means of improving the interface strength significantly is by chemically modifying the surface of nanotube to cause strong interactions between the matrix and nanotubes.

We now study the interaction between CNT-matrix when they are chemically bonded using MD simulations of single fiber pullout tests. The boundary conditions applied for the pullout test simulation are shown schematically in the Fig. 9. The corner atoms of the hydrocarbon attachments are fixed indicating that they are connected to ma-

trix at those locations. This indicates that all the stress transferred from the nanotube to the interface chemical attachments is completely transmitted to the matrix and hence represents an ideal strong interface. Displacement of  $0.05 \text{ \AA}$  is applied to the atoms at one end of the nanotube, about  $15 \text{ \AA}$  in length in order to simulate the effect of pullout. Following each displacement, the system is equilibrated for 2000 time steps of  $0.2 \text{ fs}$  duration. The simulations were carried out until some of the hydrocarbon chains fail. Typically, simulations were carried out for up to a million time steps. Variations in the length and density (number per unit area) of chemical attachments are investigated for a (10,10) CNT  $122 \text{ \AA}$  in length. The reaction force on the fixed atoms is monitored throughout the simulation and is averaged over 100 time steps before applying the next set of displacements.

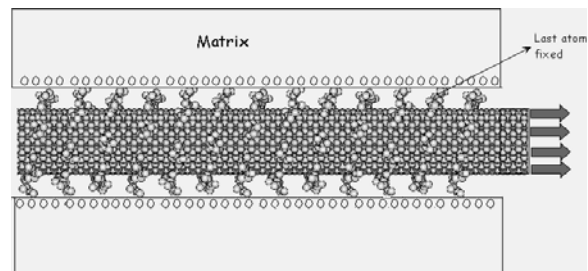


Figure 9: Schematic of the boundary conditions applied in the pullout test simulation.

Fig. 10 shows typical force vs. displacement for any hydrocarbon attachment. The force in the figure is the average (over 100 time steps) reaction force experienced by the fixed atom in the direction along the length of nanotube and corresponds to shear. Displacement is calculated as the change in the position experienced by the atom that is initially attached to the CNT. Though there are statistical variations for different chemical attachments, the general shape of the force displacement plot is as shown in Fig. 10.

The initial region of curve is flat (parallel to displacement axis) marked as region (a). This region corresponds to stretching of the hydrocarbon attachment. The flat region shows that there is minimal load transfer in this portion of curve and

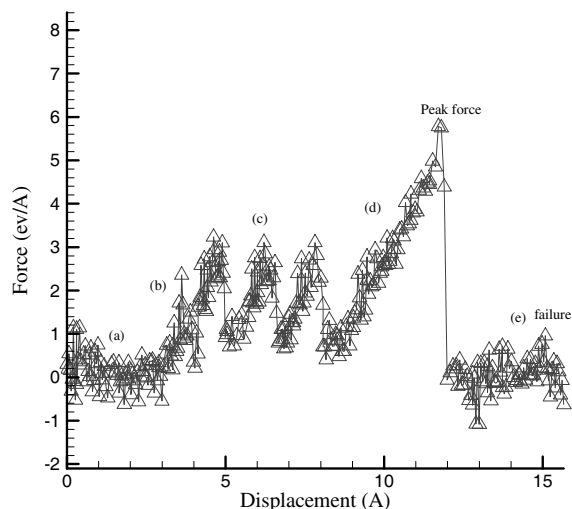


Figure 10: Reaction-force vs displacement for a typical hydrocarbon attachment for interface with 85 chemical attachments.

is similar to the mechanical analogue of a loose string becoming taut. The length of this flat portion is directly dependant on the length of hydrocarbon chain i.e. the flat region (a) is longer for hydrocarbon chains with four and five carbon atoms than for the chains with two carbon atoms. After this flat region, there is a gradual increase in the reaction force corresponding to region (b) of the curve. In this part, the functional attachment contributes to the load transfer from CNT to matrix and vice versa. Though there are statistical variations from plot to plot, the typical force experienced in this portion of the curve is about  $3\text{eV}/\text{\AA}$  ( $4.8\text{ nN}$ ). This value of force is very small but it must be noted that the area on which this force acts is of the order of  $2^2$ , and, consequently, the resulting shear stress is very high. Region (c) of the plot as shown consists of fluctuations in the reaction force. This is due to an interesting behavior of bond separation and rejoining with adjacent atoms; when the separation occurs there is a sudden drop in force but this is followed by rejoining of the hydrocarbon chain with adjacent atom of the CNT. After the jagged region, there is a steady increase in reaction force as shown in region (d) of the figure followed by total failure. The force at which the failure occurs is about  $6\text{eV}/\text{\AA}$  ( $\sim 10\text{ nN}$ ). This is the force required to break one chemi-

cal attachment; the overall force required to break all the chemical attachments is much higher and is the sum of all individual reaction forces.

The interfacial strength caused by chemical reaction is much greater than that due to non bonded interactions. This can be understood by comparing the interaction energies in both the cases. The area under the force-displacement curve denotes the energy required for detaching the hydrocarbon group from CNT. This area under the force displacement curve is about  $20\pm 4\text{ eV}$  for various attachments. The energy required to completely pullout a 122 Å (10,10) nanotube from a bundle or polyethylene matrix is about  $25\text{ eV}$  (based on Fig. 8). It can be noted that the interaction energy caused by a single chemical attachment is of the same order as that of non bonded interactions for the entire length of nanotube. The interfacial strength caused by multiple chemical attachments is significantly high.

The debonding-rebonding behavior observed in pullout test is unique to nanoscale and is generally not observed in conventional composites at macroscopic scale. Macroscopic fracture is generally considered irreversible, i.e., the energy required in the creation of a new surface during fracture is not equal to the energy required to join two surfaces and heal the damage. At atomic scale, fracture is defined as breaking of chemical bonds. The energy to form a chemical bond or break the same bond is given by the bond energy. This energy depends on the nature of bond and the species involved. However, the availability of energy is a necessary but not a sufficient condition; the kinetics of bonding process will be dictated by other factors including the electronic state of the atomic neighborhood, the temperature and the gradient of potential energy as well. The energy required to break two bonds is exactly equal to the energy released to join the same two atoms to form chemical bond. Whether two atoms will join to form a chemical bond is determined based on the distance between the atoms and the kinetics of the process.

Different cases are considered with varying number of chemical attachments. For the (10,10) CNT studied earlier, there will be 85 chemical attach-

ments if one chemical attachment exists attached per repeat unit of the CNT excluding the end of CNT that is subject to displacements. Different number of chemical attachments 85, 45, 20, 10 and 5 are placed at circumferentially random and longitudinally equidistant locations and pullout tests simulated with all the other variables such as temperature and displacement rate maintained constant.

The general shape of force-displacement curve remains similar to that shown in Fig. 10. The values of points of inflexion also remain similar within the statistical variation, but there is a tendency for the de-bonding and rebonding region to be prolonged, when the density of chemical attachments is lowered. For example, in the case of 5 and 10 chemical attachments, we observed that there is extended bonding and rebonding behavior but no failure of either the interface or the fiber. However, in the case of 85 or 45 chemical attachments we observed that the interface failure (fracture of chemical attachments) occurs as shown in Fig. 10; this is followed by the fracture of the nanotube.

Fig. 11 shows that the normal stress in the nanotube vs applied displacement for different interfacial bond strengths (i.e. numbers of chemical attachments). The stress is calculated as the net force experienced by the region of nanotube on which the displacement is applied, divided by the cross sectional area. As can be seen from Fig. 11, when the interface consists of low number of chemical attachments, the stress in nanotube stabilizes to a certain value, for e.g. 30 GPa, in nanotube with 5 chemical attachments. This stabilizing coincides with the fact that there is a continuous bonding-rebonding behavior and no failure observed in such interfaces. This indicates that the interface corresponding to 5 chemical attachments induces a stress of 30 GPa in the nanotube. Because of the debonding-rebonding behavior a steady state is reached in the load borne by the fiber. This stress in the fiber increases with the strength of the interface i.e., the number of chemical attachments. For example, interface with 10 chemical attachments induces stress of about 50 GPa. When the number of chemical attachments

is very high, the stress in the interfacial region as well as that in the fiber reaches the stress to failure causing failure in the interface and the fiber. The bonding-debonding behavior suggests a possibility of designing the interfaces for nanocomposites for a specific level of load carrying capacity.

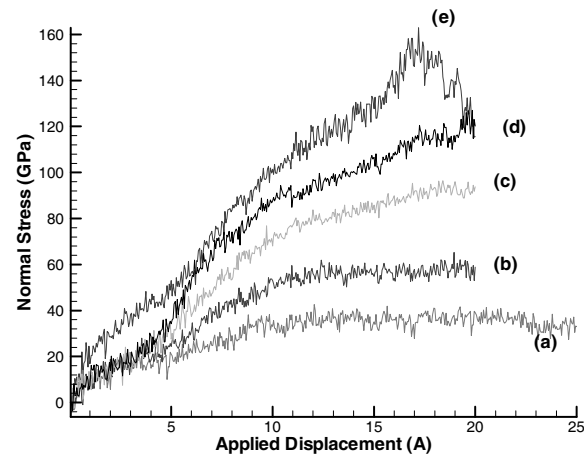


Figure 11: Normal stress experienced by carbon nanotube during pullout test for different number of chemical attachments (a) 5, (b) 10, (c) 25, (d) 45 and (e) 85. The circle at curves (d) and (e) marks the region where failure of chemical attachments is observed, while there is no failure in plots (a) and (b).

As noted this interface behavior represents the upper bound force capacity since the matrix end of the attachment is assumed to be completely fixed. The computational effort for this realistic case is very high and would not have been possible but for the effective parallelization of the code. In the next section, we explicitly model the behavior of matrix and consider the effect of processing on interfacial behavior.

#### 4 Matrix and Processing Considerations on Interface Behavior

In order to use functionalized CNTs in composites the typical route may consist of chemical treatment for functionalization of nanotubes followed by composite processing to make the composites (e.g. Gonjy 2004, Pavia 2004). For good interface strength, it is essential that the surface at-

tachments on functionalized CNTs be chemically bonded with the matrix. MD simulations can be used to study the processing of CNT based polymer composites, where the bond formation at the interfaces occurs based on energetics and kinetics.

The matrix is modeled as a crystalline hydrocarbon polymer composed of 48 polymer chains oriented parallel to the nanotube. The polymer consists of (i) Polyethylene ( $-\text{CH}_2-\text{CH}_2-$ )<sub>n</sub> and (ii) polythene with considerable number of unsaturated bonds ( $-\text{CH}=\text{CH}$ ). A 122 Å (10,10) carbon nanotube functionalized with 85 butene chemical attachments is at the center of the polymer matrix as shown in Fig. 12a. These composite systems consist of about  $10^4$  to  $1.2 \times 10^4$  atoms. There are no chemical bonds between the matrix and the attachments on the nanotube initially. The composite is then subject to thermal processing at 500K as shown in Fig. 12(b). This thermal processing is expected to facilitate chemical bonding at the interface and thereby improve the interface strength. We observe that after equilibration, about six chemical bonds are formed in the polymer system with unsaturated bonds whereas one chemical bond is formed in the saturated polythene matrix system. Further, considerable tangling between the matrix and nanotube chemical attachments is also observed.

The interface strength is now studied on the composite systems by the pullout simulation of nanotube from matrix. All the atoms of the outer layers of the polymer chains and atoms at the ends of all polymer chains are fixed (see inset in Fig. 13). Displacements are applied to the atoms at one end of nanotube and the forces are monitored. The normal stress calculated from these applied forces is plotted in Fig. 13. Plot (a) in Fig. 13 corresponds to the case when there are unsaturated bonds in the matrix and plot (b) corresponds to polyethene matrix. For comparison, the normal stress obtained by fixing the chemical attachments (section 3) for interfaces of 85 and 5 chemical attachments are shown in plot (c) and plot (d). It is clear that unsaturated matrix resulting in a six chemical bonds at the interface, definitely has higher interface strength than the saturated polythene matrix. Further the tangling

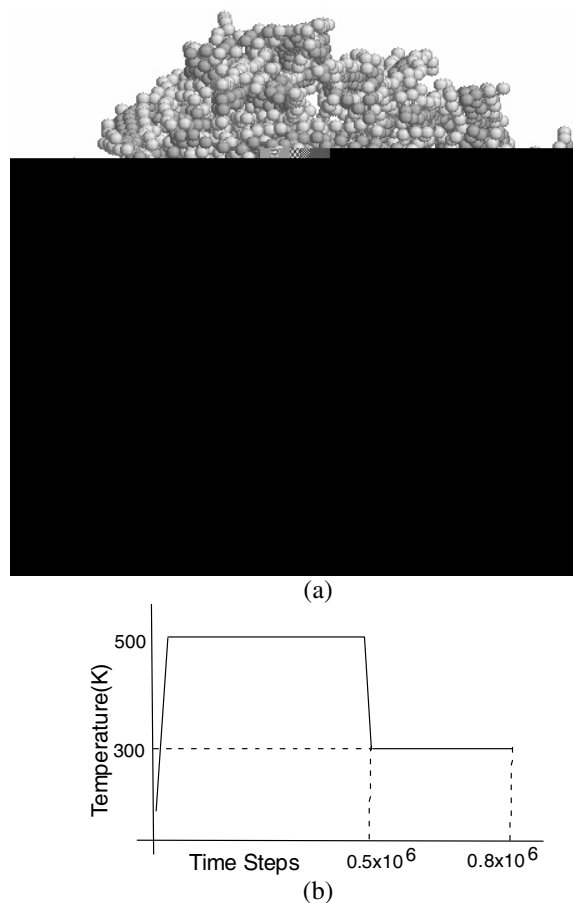


Figure 12: (a) Simulation snapshot of carbon nanotube-polyethene composite during the thermal processing. (b) Thermal processing applied to the composite system.

between functional attachments and the matrix does not seem to contribute towards the interface strength compared to strengthening due to chemical bonding. Debonding-rebonding which was significantly observed when the chemical attachments are fixed is still observed in the presence of matrix but to a much lesser extent. Most of chemical bonds at the interface fail before debonding-rebonding is experienced.

It is clear that the load transfer is significantly influenced by the chemical bonding compared to any other type of non-bonded interactions (intertwining or Van Der Waals interactions). The natural question then is what promotes chemical bonding. Obviously providing unsaturated chemical bonds compared to saturated chemical bonds en-

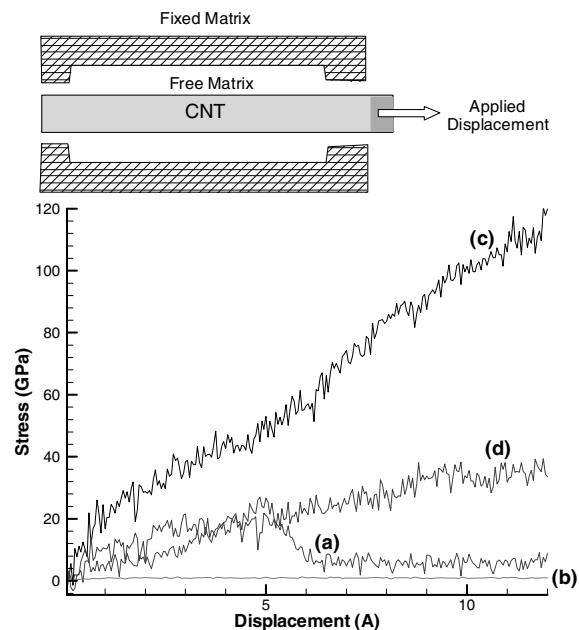


Figure 13: Normal stress experienced by carbon nanotube during pullout test (a) polymer matrix with unsaturated bonds (b) polythene matrix (c) 85 chemical attachments fixed at corners and (d) 5 chemical attachments fixed at corners. Inset shows the schematic of boundary conditions.

hances the possibility. Further neat CNT by themselves show very little tendency to form chemical bonds. The choice of functional groups that can easily react with CNTs on one side and matrix on the other end can improve the bond strength.

## 5 Summary

Parallel MD and statics simulations are used to study the interfacial behavior in CNT composites. An algorithm based on sorting the projected image is used for domain decomposition, specifically exploiting the fact that CNTs in general lie along a preferred orientation. We achieve a speedup of 8.6 on 16 processors. Parallelization aids in solving the computationally intensive problem and has been the developed algorithm can be used in a number of other solution methods. The parallel MD simulations are then used to simulate the processing of CNTs with two types of polymers with saturated and unsaturated bonds results in interfaces with different levels of inter-

face strength. Some additional conclusions of the study are as follows:

1. Interface strength is very low (few MPa) when it is based on long range Van Der Waals interactions only. This can be appreciably improved to few GPa by chemically modifying the nanotube surface.
2. The stress experienced by the nanotube increases with interface strength (number of chemical attachments). When the number of chemical attachments is very high, it results in failure at interface and/or nanotube. Lower number of chemical attachments result in a steady state of extended debonding-rebonding behavior akin to macroscopic stick-slip behavior.
3. Formation of chemical bonds (and hence increased interface strength) can be enhanced by using functionalized CNT in polymer matrix with unsaturated bonds.

**Acknowledgement:** We gratefully acknowledge partial funding provided Army Research Office (Grant # DAAD19-02-1-0376), National Security Agency (Grant # H98230-04-c-0499) and National Science Foundation (Grant # CMS-0403746) during various phases of this research.

## References

- Ajayan, P.M.; Schadler, L.S.; Giannaris, C.; Rubio, A. (2000): Single-walled carbon nanotube-polymer composites: strength and weakness. *Advanced Materials*, 12, 750.
- Allaouia, A.; Baia, S.; Cheng, H.M.; Baia, J.B. (2002): Mechanical and electrical properties of a MWNT/epoxy composite, *Composites Science and Technology*, 62, 1993-1998.
- Ananth, C.R.; Chandra, N. (1995): Numerical modeling of fiber pushout testing metallic ceramic and intermetallic matrix composites - Mechanics of the failure processes, *Journal of Composite Materials*, 29, 1488-1499.
- Andrews, R.; Jacques, D.; Rao, A.M.; Rantell, T.; Derbyshire, F.; Chen, Y.; Chen, J.; Haddon,

- R.C.** (1999): Nanotube composite carbon fibers, *Applied Physics Letters*, 75, 1329-1331.
- Andrews, R.; Jacques, D.; Minot, M.; Rantell, T.** (2002): Fabrication of carbon multiwalled nanotube/polymer composites by shear mixing, *Macromolecular Materials and Engineering*, 287, 395-400.
- Bin, Y.; Kitanaka, M.; Zhu, D.; Matsuo, M.** (2003): Development of highly oriented polyethylene filled with aligned carbon nanotubes by gelation/crystallization from Solutions, *Macromolecules*, 36, 6213-6219.
- Brenner, D.W.** (1991): Empirical potential for hydrocarbon for use in simulating the chemical vapor deposition of diamond films. *Physical Review B*, 42, 9458.
- Brenner, D.W.; Shenderova, O.A.; Harrison, J.A.; Stuart, S.J.; Ni, B.; Sinnott, S.B.** (2002): A second-generation reactive empirical bond order (REBO) potential energy expression for hydrocarbons, *Journal of Physics-Condensed Matter*, 14, 783-802.
- Caglar, A.; Griebel, M.** (2000): *On the numerical simulation of Fullerene nanotubes: C<sub>100,000,000</sub> and beyond*. Molecular dynamics on parallel computers, Editors: R. Esser, et. al., World Scientific.
- Carman, G.P.; Averill, R.C.; Reifsnider, K.L.; Reddy, J.N.** (1993): Optimization of Fiber Coatings to Minimize Stress-Concentrations In Composite-Materials, *Journal of composite materials*, 27, 589-606.
- Chandra, N.; Namilaie, S.; Shet, C.** (2004): Local elastic properties of carbon nanotubes in the presence of Stone -Wales defects, *Physical Review B*, 69, 094101.
- Chandra, N.; Li, H.; Shet, C.; Ghonem, H.** (2002): Some issues in the application of cohesive zone models for metal ceramic interfaces, *International Journal of Solids and Structures*, 39, 2827-2835.
- Chen, J.; Hamon, M.A.; Hu, H.; Chen, Y.; Rao, A.M.; Eklund, P.C.; Haddon, R.C.** (1998): Solution properties of single-walled carbon nanotubes, *Science*, 282, 95-98.
- Cooper, C.A.; Young, R.J.; Halsall, M.** (2001): Investigation into the deformation of carbon nanotubes and their composites through the use of Raman spectroscopy, *Composites: Part A*, 32, 401-411.
- Cooper, C.A.; Cohen, S.R.; Barber, A.H.; Wagner, H.D.** (2002): Detachment of nanotubes from a polymer matrix. *Applied Physics Letters*, 81, 3873-3875.
- Demczyk, B.G.; Wang, Y.M.; Cumings, J.; Hetman, M.; Han, W.; Zettl, A.; Ritchie, R.O.** (2002): *Materials Science and Engineering A*, 334, 173-178.
- Girifalco, L. A.; Hodak, M.; Lee, R.** (2000): Carbon nanotubes, buckyballs, ropes, and a universal graphitic potential. *Physical Review B*, 62, 13104.
- Gojny, F.H.; Wichmann, M.H.G.; Kopke, U.; Fiedler, B.; Schulte, K.** (2004): Carbon nanotube-reinforced epoxy-composites: enhanced stiffness and fracture toughness at low nanotube content, *Composites Science and Technology*, 64, 2363-2371.
- Gong, X.; Liu, J.; Baskaran, S.; Voise, R.D.; Young, J.S.** (2001): Surfactant-assisted processing of carbon nanotube/polymer composites, *Chemistry of Materials*, 12, 1049-1052.
- Jia, Z.; Wang, Z.; Xu, C.; Liang, J.; Wei, B.; Wu, D.; Zhu, S.** (1999): Study on poly (methyl methacrylate) carbon nanotube composites, *Materials Science and Engineering A*, 271, 395-400.
- Khare, B.N.; Meyyappan, M.; Cassell, A.M.; Nguyen, C.V.; Han, J.** (2002): Proton irradiation of carbon nanotubes, *Nano letters*, 2, 73-75.
- Ling, X.; Atluri, S. N.** (2006): A lattice-based cell model for calculating thermal capacity and expansion of single wall carbon nanotubes, *CMES: Computer Modeling in Engineering and Sciences*, 14, 2, 91-100.
- Ma, J.; Lu, H.; Wang ,B.; Hornung, R.; Wissink, A.; Komunduri, R.** (2006): Multiscale simulation using Generalized Interpolation Material Point (GIMP) Method and Molecular Dynamics (MD), *CMES: Computer Modeling in Engineering and Sciences*, 14, 2, 101-118.

**Michelson, E.T.; Huffman, C.B.; Rinzler, A.G.; Smalley, R.E.; Hauge, R.H.; Margrave, J.L.** (1996): Fluorination of single-wall carbon nanotubes, *Chemical Physics Letters*, 296, 188-194.

**Namilae, S.; Chandra, N.** Role of atomic scale interfaces in the compressive behavior of carbon nanotubes in composites, *Composite Science and Technology*, (In Print).

**Namilae, S.; Chandra, N.; Shet, C.** (2004): Mechanical behavior of functionalized nanotubes, *Chemical Physics Letters*, 387, 247-252.

**Namilae, S.; Chandra, N.** (2005): Multiscale model to study the effect of interfaces in carbon nanotube based composites, *Journal of Engineering materials and technology*, 127, 222-232.

**Park, J.Y.; Cho, Y-S.; Kim, S.Y.; Jun, S.; Im, S.** (2006): A quasicontinuum method for deformations of carbon nanotubes, *CMES: Computer Modeling in Engineering and Sciences*, 11, 2, 61-72.

**Pekker, S.; Salvetat, J.P.; Jakab, E.; Bonard, J.M.; Forro, L.** (2001): Hydrogenation of Carbon Nanotubes and Graphite in Liquid Ammonia, *Journal of Physical Chemistry B*, 105, 7938-7943.

**Paiva, M.C.; Zhou, B.; Fernando, K.A.S.; Lin, Y.; Kennedy, J.M.; Sun, Y.P.** (2004): Mechanical and morphological characterization of polymer-carbon nanocomposites from functionalized carbon nanotubes, *Carbon* 42, 2849-2854.

**Qian, D.; Dickey, E.C.; Andrews, R.; Rantell, T.** (2000): Load transfer and deformation mechanisms in carbon nanotube-polystyrene composites, *Applied Physics letters*, 76, 2868-2870.

**Saito, R.; Dresselhaus, G.; Dresselhaus, M.S.** (2001): *Physical properties of carbon nanotubes*, Imperial College Press.

**Srivastava, D.; Barnard, S.T.** (1997): Molecular dynamics simulation of large-scale Carbon nanotubes on shared-memory architecture, *Proceedings of SC1997, IEEE*.

**Schadler, L.S.; Giannaris, S.C.; Ajayan, P.M.** (1998): Load transfer in carbon nanotube epoxy composites, *Applied Physics Letters*, 73, 26, 3842-3844.

**Tang, W.; Santare, M.H.; Advani, S.G.** (2003):

Melt processing and mechanical property characterization of multi-walled carbon nanotube/ high density polyethylene (MWNT/HDPE) composite films, *Carbon*, 41, 2779-2785.

**Treacy, M.M.J.; Ebbesen, T.W.; Gibson, J.M.** (1996): Exceptionally high Young's modulus observed for individual carbon nanotubes, *Nature*, 381, 678-680.

**Yakobson, B.I.; Brabec, C.J.; Bernholc, J.** (1996): Nanomechanics of carbon tubes: Instabilities beyond linear response, *Physical Review letters*, 76, 2511-2514.